AAC Journals.ASM.org

Population Pharmacokinetics and Target Attainment of Meropenem in Plasma and Tissue of Morbidly Obese Patients after Laparoscopic Intraperitoneal Surgery

Mathias Wittau,[a] Jan Scheele,[a] Max Kurlbaum,[b] Claas Brockschmidt,[a]* Anna M. Wolf,[a] Evelyn Hemper,[a] Doris Henne-Bruns,[a] Jürgen B. Bulitta[c]*

Department of Visceral Surgery, University of Ulm, Ulm, Germany[a]; Department of Clinical Chemistry, University of Ulm, Ulm, Germany[b]; Drug Delivery, Disposition and Dynamics, Monash Institute of Pharmaceutical Sciences, Monash University (Parkville Campus), Parkville, Victoria, Australia[c]

Meropenem serves as a clinically important, broad-spectrum antibiotic. While meropenem is commonly used in obese patients, its pharmacokinetics in this patient group is not well known. Our aim was to characterize the population pharmacokinetics and target attainment in plasma, subcutaneous tissue, and peritoneal fluid for meropenem in morbidly obese patients. Four doses of 1g meropenem were given as 15-min infusions every 8 h to five morbidly obese patients (body mass index [BMI], 47.6 to 62.3 kg/m^2). After the fourth dose, serial meropenem concentrations were determined in plasma and, via microdialysis, in subcutaneous tissue and peritoneal fluid. All concentrations were analyzed simultaneously via population modeling, and target attainment probabilities predicted via Monte Carlo simulations using the target of unbound meropenem concentrations above the MIC for at least 40% of the dosing interval. For patients with 53 kg fat-free mass, total clearance was 18.7 liters/h and volume of distribution at steady state was 27.6 liters. The concentrations in subcutaneous tissue and peritoneal fluid largely paralleled those in plasma (equilibration half-life, <30 min). The area under the curve (AUC) in subcutaneous tissue divided by the plasma AUC had a mean of 0.721. For peritoneal fluid, this AUC ratio had a mean of 0.943. Target attainment probabilities were >90% after 1 g meropenem every 8 h as a 15-min infusion for MICs of up to 2 mg/liter in plasma and peritoneal fluid and 0.5 mg/liter in subcutaneous tissue. Meropenem pharmacokinetics in plasma and peritoneal fluid of obese patients was predictable, but subcutaneous tissue penetration varied greatly. (This study has been registered at ClinicalTrials.gov under registration no. NCT01407965.)

While antimicrobial resistance is one of the greatest threats to human health, the number of new antibiotics against multidrug-resistant bacteria declined drastically over the last 3 decades (1–3). Meropenem continues to serve as an important component of our antibiotic armamentarium and covers a large range of clinically relevant pathogens for antibiotic therapy, including those causing intra-abdominal infections or infections of the subcutaneous tissue. Meropenem is a potent, broad-spectrum β-lactam antibiotic that yields relatively rapid bacterial killing and is among the first antibiotic options for treatment of severe infections; it covers most of the pathogens relevant for intra-abdominal infections (4). Meropenem is a hydrophilic molecule, and it is unknown whether meropenem penetrates well into the subcutaneous tissue and peritoneal fluid of obese patients.

Obese patients are at a high risk of postoperative and hospital-related infections (5), and optimal management of these infections is crucial to improve the outcome of obese patients with severe infections. The selection of the antibiotic and dose are critical to manage those infections (5, 6). Recommended daily doses are based on pharmacokinetic/pharmacodynamic (PK/PD) studies usually conducted in nonobese healthy volunteers (5). However, PK variables may differ in obese and nonobese patients, potentially resulting in inadequate antibiotic plasma and tissue concentrations. Thus, PK studies in obese, noninfected individuals are essential to avoid the risk of over- or underdosing.

Only a few studies have assessed the PK of meropenem in obese patients (4–8), and some of these studies found considerably different clearances and volumes of distribution in obese and nonobese patients. These studies did not perform population pharmacokinetic modeling and did not assess the peritoneal fluid and subcutaneous tissue penetration of meropenem in obese patients.

As meropenem is a hydrophilic molecule, it is important to determine whether its PK is predictable in morbidly obese patients. If the between-subject variability (BSV) of clearance and volume of distribution can be predicted based on total body weight (WT) or fat-free mass (FFM), this would allow us to more precisely achieve target concentrations and PD targets in obese patients. A PD target of unbound carbapenem plasma concentrations above the MIC ($fT_{>MIC}$) for at least 40% of the dosing interval has been shown to predict near-maximal bacterial killing at 24 h in mice (9, 10).

Received 3 February 2015 **Returned for modification** 5 April 2015
Accepted 19 July 2015

Accepted manuscript posted online 27 July 2015

Citation Wittau M, Scheele J, Kurlbaum M, Brockschmidt C, Wolf AM, Hemper E, Henne-Bruns D, Bulitta JB. 2015. Population pharmacokinetics and target attainment of meropenem in plasma and tissue of morbidly obese patients after laparoscopic intraperitoneal surgery. Antimicrob Agents Chemother 59:6241–6247. doi:10.1128/AAC.00259-15.

Address correspondence to Mathias Wittau, mathias.wittau@uniklinik-ulm.de.

* Present address: Claas Brockschmidt, Department of Surgery B, Evangelisches Krankenhaus, Hagen, Germany; Jürgen B. Bulitta, University of Florida, College of Pharmacy, Center for Pharmacometrics and Systems Pharmacology, Orlando, Florida, USA.

M.W. and J.S. contributed equally to this work.

doi:10.1128/AAC.00259-15

Our primary objective was to characterize the population pharmacokinetics of meropenem in plasma, subcutaneous tissue, and peritoneal fluid of morbidly obese, noninfected individuals. As the second objective, we evaluated whether clearance and volume of distribution can be predicted by total body weight or fat-free mass. Finally, we sought to predict the probability of target attainment via Monte Carlo simulations.

MATERIALS AND METHODS

Study design. This prospective, monocentric, open-label study was conducted at the University of Ulm, Department of Visceral Surgery, from August 2012 to January 2013 (meropenem arm; registered at ClinicalTrials.gov under registration no. NCT01407965). The ethics committee of the University of Ulm and The Federal Institute for Drug and Medical Devices of Germany approved the protocol, and prior written informed consent was obtained from all study participants. The trial was conducted in accordance with the revised version of the Declaration of Helsinki and current revisions of the Good Clinical Practice Guidelines of the European Commission.

Patient population. We included noninfected, hospitalized patients with an age of at least 18 years and body mass index (BMI) of at least 40 kg/m^2 who required surgical intervention (open or laparoscopic surgery) at intra-abdominal organs. Exclusion criteria were as follows: pregnancy or lactation in women; emergency surgery; history of serious allergy or intolerance to β-lactam antibiotics; systemic antimicrobial therapy with ceftazidime within 7 days prior to study entry; ongoing intra-abdominal infections; terminal illness; severe diseases of the liver, e.g., cirrhosis of the liver with alanine aminotransferase (ALT) or aspartate transaminase (AST) >6× the upper limit of normal (ULN) and bilirubin >3× the ULN; severe renal insufficiency with a creatinine clearance of ≤30 ml/min; neutrophil count of <1,000 cells/mm^3; platelet count of <75,000 cells/mm^3 and coagulation measures (international normalized ratio [INR]) of >1.5× ULN; ongoing chemotherapy and/or radiotherapy; and concurrent medication with valproic acid.

Dosing. All patients received 1 g meropenem every 8 h (Meronem, license no. 8592.02.00; AstraZeneca, Inc., Wedel, Germany) intravenously on the day of surgery. All doses were given as a 15-min intravenous infusion. The fourth dose of meropenem, administered on day 1 after surgery, was used for sample collection up to 8 h after administration. This dose was administered after the microdialysis recovery procedure and wash-out of the microdialysis probes (see below).

Microdialysis. Samples of subcutaneous adipose interstitial space fluid and peritoneal fluid were collected using microdialysis. During the surgical procedure, a microdialysis probe was placed in the subcutaneous tissue of the abdominal wall (CMA 63; Mdialysis, Stockholm, Sweden), while a second microdialysis probe was placed into the abdominal cavity before closure (CMA 62; Mdialysis, Stockholm, Sweden). The probes were calibrated using the retrodialysis technique (11). The probes were perfused with lactated Ringer's solution for 24 h at a flow rate of 2 μl/min. Eight hours after the third dose of meropenem, the catheters were perfused with 20 mg/liter meropenem in lactated Ringer's solution for 60 min. A sample was collected during the last 25 min of the retrodialysis procedure, and the recovery (%) calculated as $100 \cdot (1 - C_{dialysate}/C_{perfusate})$, where $C_{perfusate}$ is the initial solution concentration entering the microdialysis probe and $C_{dialysate}$ the concentration of the solution leaving the probe (11). Calibration was followed by a wash-out period with blank lactated Ringer's solution for at least 60 min. Microdialysis samples were taken over a time period of 25 min at 30, 60, 120, 180, 300, and 480 min after meropenem administration. The flow rate was kept at 2 μl/min. Microdialysis samples were stabilized (see below) with 2-(4-morpholino)ethanesulfonic acid (MES) (0.1 M, pH 6.5, 1:1), immediately frozen, and stored at −80°C until analysis.

Blood sampling. Blood samples were taken at the same times as the microdialysis samples. Blood samples were immediately cooled in an ice-water bath. Plasma was obtained by centrifugation of blood samples at 4,000 rpm for 10 min at 4°C. Plasma samples were stabilized immediately after sampling using MES buffer (100 mM, pH 6.5, 1:1 [vol/vol]) that was added to the plasma samples. Matrix controls, internal standards, calibration curve standards, and pharmacokinetic samples were immediately frozen and stored at −80°C until analysis.

Meropenem assay. Water and methanol (liquid chromatography-mass spectrometry [LC-MS] grade) were purchased from VWR (Darmstadt, Germany), and acetic acid, ammonium acetate, MES (0.1 M, pH 6.5), and meropenem from Sigma-Aldrich (Steinheim, Germany). The internal standard (meropenem-D_6) was received from Toronto Research Chemicals (Toronto, Canada). Mobile phase A for high-performance liquid chromatography (HPLC) analysis consisted of water with 2 mM ammonium acetate (NH_4OAc), 0.1% acetic acid, pH 3.8, and mobile phase B of methanol. The plasma and dialysate preparations were performed according to the method of Koal et al. (12).

A volume of 10 μl methanolic meropenem-D_6 (final concentration, 10 mg/liter) as an internal standard was added to every sample. The HPLC system consisted of two pumps (LC 20 AD), an autosampler (SIL 20 AC HT), and an oven (CTO-20 AC) from Shimadzu (Duisburg, Germany). Prepared samples were kept at 4°C in the autosampler until analysis. The injection volume was 10 μl.

Chromatography was performed with an XBridge column (C_{18}, 2.5-μm particle size, 3.0 by 75 mm; Waters, Milford, MA) in combination with an XBridge guard cartridge (C_{18}, 2.5-μm particle size, 3.0 by 20 mm). Separation was performed with a linear gradient (total flow, 0.5 ml/min) from 95% phase A, 5% phase B at time zero to 10% phase A, 90% phase B at 4 min, followed by a second gradient from 10% phase A, 90% phase B at 4 min to 95% phase A, 5% phase B at 6 min. The system was reequilibrated for 3 min before the next injection.

The MS experiments were performed with an API 3200 triple-quadrupole (AB Sciex, Framingham, MA) in positive electrospray ionization (ESI) mode. The following settings were applied: capillary voltage, 5.0 kV; temperature, 675°C; curtain gas, 20 lb/in^2; collisionally activated dissociation gas, 6 lb/in^2; gas 1 and 2, 55 lb/in^2; declustering potential, 41 V; and entrance potential, 5 V. For meropenem, the transitions *m/z* 384.1→*m/z* 141.2 as quantifier and *m/z* 384.1→*m/z* 254.2 as qualifier in multireaction monitoring (MRM) mode were used. For the internal standard meropenem-D_6, the transition was *m/z* 390.1→*m/z* 147.2. Quantification was processed with Analyst software (version 1.5.2) with linear regression, origin excluded, and 1/*x* weighting.

The limit of quantification (signal-to-noise ratio >10) for plasma and dialysate was 0.1 mg/liter. The assay was linear from 0.1 to 100 mg/liter, with r^2 values of 0.992 for dialysate and 0.998 for plasma. The interday precision ranged from 7.2 to 13.2% for dialysate and from 2.3 to 6.1% for plasma. The intraday precision ranged from 1.6 to 3.5% for dialysate and from 4.1 to 13.9% for plasma. The accuracy was found to be from 91.5 to 107.6% for plasma and from 102.2 to 107.4% for dialysate. Five replicates with three meropenem concentrations (1, 50, and 100 mg/liter) were used to determine precision and accuracy.

Population modeling and Monte Carlo simulations. (i) Structural model. We considered linear models with one or two disposition compartments to describe the PK of meropenem in plasma. The time course of unbound meropenem concentrations in subcutaneous tissue and peritoneal fluid was described by multiplying the concentration in the central or peripheral compartment with a factor (F_{SC} for subcutaneous tissue and F_{PF} for peritoneal fluid) such as we described previously (13). The F_{SC} and F_{PF} represent the ratios for the area under the curve (AUC) between the respective peripheral site and plasma.

Additional models were studied for which subcutaneous tissue and peritoneal fluid were described by additional compartments with a small volume of distribution (fixed to 0.1 liter), as we described previously (14). The small volume of distribution (0.1 liter) was chosen to not affect the overall PK behavior of meropenem. This additional analysis allowed us to determine whether subcutaneous tissue and peritoneal fluid were kinetically more similar to the central or peripheral compartment.

TABLE 1 Demographic characteristics

Characteristic	Mean value ± SD	No. or median (range)
Sex		2 male, 3 female
Age (yr)	40.0 ± 7.87	39 (31–49)
Weight (kg)	158 ± 33.5	163 (116–203)
Fat-free mass (kg)	72.5 ± 19.8	63.8 (52.3–94.0)
Height (cm)	170 ± 14.5	163 (155–190)
Body mass index (kg/m^2)	54.2 ± 7.02	51.9 (47.6–62.3)
Body surface area (m^2)	2.72 ± 0.390	2.72 (2.23–3.19)
Serum proteins (g/liter)	71.0 ± 6.67	72.0 (62.0–79.0)
Serum creatinine (μmol/liter)	73.0 ± 5.96	75.0 (64.0–80.0)
Albumin (g/liter)	42.8 ± 1.79	43.0 (41.0–45.0)

(ii) Parameter variability model and covariate effects. Between-subject variability (BSV) was described by an exponential parameter variability model for all parameters. Given the small sample size of our study, we did not perform empirical covariate model building. Instead, we applied standard allometric scaling to estimate whether body size (i.e., WT or FFM) could predict clearances and volumes of distribution. We considered FFM (15) to account for the significantly altered body composition of morbidly obese patients in comparison to that of healthy volunteers.

(iii) Estimation. The model parameters were estimated simultaneously using all meropenem concentrations in plasma, subcutaneous tissue, and peritoneal fluid via the importance sampling algorithm (pmethod = 4) in parallelized S-ADAPT (version 1.57) (16). The analysis was facilitated by the SADAPT-TRAN tool (17, 18). Competing models were assessed by the objective function (−1 × log-likelihood), plausibility of the parameter estimates, standard diagnostic plots, visual predictive checks, and normalized prediction distribution error plots, as described previously (19–21). Noncompartmental analysis was performed using the linear-up/log-down trapezoidal rule as implemented in WinNonlin Professional (version 5.3; Pharsight, Cary, NC).

(iv) Monte Carlo simulations. Using the final population PK model, we performed Monte Carlo simulations to predict the time courses of meropenem concentrations in plasma, subcutaneous tissue, and peritoneal fluid of morbidly obese patients. In these simulations, 1 g meropenem was simulated as a 15-min or 3-h infusion every 8 h or as a continuous infusion of 3 g/day (with a 1-g loading dose). We simulated morbidly obese patients with the same FFM as those in the present study (geometric mean FFM, 70.3 kg; 27.4% coefficient of variation [CV]). The $fT_{>MIC}$ was calculated by numerical integration at steady state using Berkeley Madonna software (version 8.3.18). The fractions of patients achieving the PK/PD targets of 40% and 75% $fT_{>MIC}$ were calculated to approximate the probability of target attainment (9, 10). The latter target has been associated with clinical cure by meropenem in febrile neutropenic patients with bacteremia (22). To account for potentially more severe infections, we additionally calculated the target attainment probability for a target of 100% $fT>MIC$ that has been previously proposed for meropenem (23). The PK/PD breakpoint was defined as the highest MIC with a probability of target attainment of at least 90%.

RESULTS

Six morbidly obese patient were included in the study. One patient's data had to be excluded from analysis due to an incorrect meropenem concentration of $C_{perfusate}$ during the recovery procedure. The body weight was 158 ± 33.5 kg (mean ± standard deviation [SD]), and the BMI was 54.2 ± 7.02 kg/m^2 (Table 1). All patients had laparoscopic intraperitoneal surgery (five laparoscopic sleeve gastrectomies and one laparoscopic hernia repair at the abdominal wall).

Without scaling of PK parameters by body size, noncompartmental analysis yielded median (range) values of 26.2 (18.8 to 35.3) liters/h for total clearance and 50.4 (28.2 to 65.8) liters for volume of distribution at steady state. The terminal half-lives were comparable at all three sites, with 1.24 (1.04 to 1.41) h in plasma, 1.16 (0.833 to 2.45) h in subcutaneous tissue (n = 4), and 1.35 (0.978 to 1.95) h in peritoneal fluid. The values (average ± SD) for observed peak concentrations 30 min after start of the last infusion were 24.6 ± 10.1 mg/liter in plasma, 24.1 ± 22.1 mg/liter in subcutaneous tissue, and 23.2 ± 10.8 mg/liter in peritoneal fluid.

The meropenem concentration profiles declined with two exponential phases (Fig. 1). When PK parameters were scaled allometrically using a standard FFM of 53 kg, total clearance was 18.7

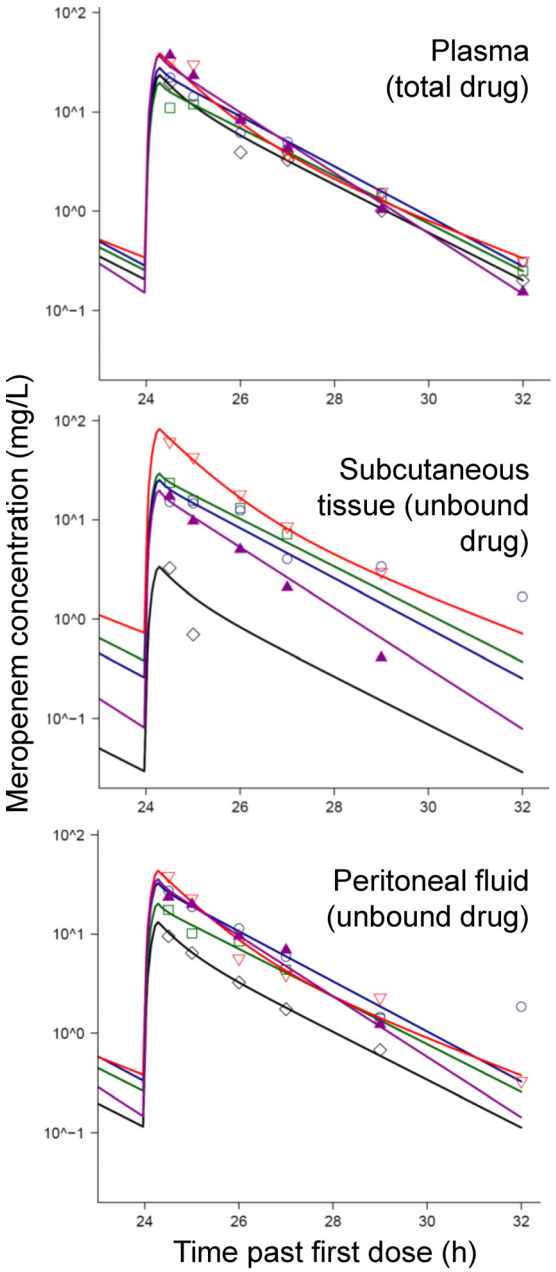

FIG 1 Observed (symbols) and individually fitted (lines) meropenem concentrations in plasma, subcutaneous tissue, and peritoneal fluid after four doses of 1 g meropenem as a 15-min infusion every 8 h.

TABLE 2 Population pharmacokinetic parameter estimates for meropenem in morbidly obese patients[a]

Parameter	Symbol	Unit	Population mean	Between-subject variability
Total clearance	CL	Liters/h	18.7[b]	0.0386[c]
Distribution clearance between central and peripheral compartments	CL_d	Liters/h	29.4[b]	1.79
Volume of distribution of central compartment	V_1	Liters	21.5[b]	0.104
Volume of distribution of peripheral compartment	V_2	Liters	6.16[b]	0.0422
Ratio of AUC values in subcutaneous tissue and plasma	F_{SC}		0.721[d]	1.12
Ratio of AUC values in peritoneal fluid and plasma	F_{PF}		0.943[d]	0.311

[a] The standard deviations of the additive and proportional residual errors were 0.0235 mg/liter and 21.6% in plasma, 1.26 mg/liter and 9.58% in SC tissue, and 0.617 mg/liter and 10.3% in peritoneal fluid. AUC, area under the concentration-time curve from time zero to infinity; SC, subcutaneous tissue; PF, peritoneal fluid.
[b] Estimates represent a patient with normal body size (i.e., 53 kg fat-free mass) and are based on an allometric body size model.
[c] Estimate represents the apparent coefficient of variation of a normal distribution on natural logarithmic scale.
[d] The half-lives of equilibration between subcutaneous tissue and plasma and between peritoneal fluid and plasma were rapid (equilibration half-life, <0.5 h). The final model assumed a very rapid equilibration between the respective peripheral site and plasma.

liters/h and volume of distribution at steady state (volume of distribution of central compartment plus volume of distribution of peripheral compartment [$V_1 + V_2$]) was 27.6 liters (Table 2). After accounting for FFM, the estimated between-subject variabilities of clearance, V_1, and V_2 were small (<11%). While distribution clearance was more varied, this had a limited impact on the plasma concentration time profiles, as equilibration between the central and peripheral compartments was relatively rapid.

In agreement with the similar terminal half-lives at all three sites, the concentrations in tissue essentially paralleled those in plasma (Fig. 1), suggesting that the equilibration half-life between subcutaneous tissue or peritoneal fluid and plasma was rapid. This was confirmed in an additional modeling analysis by estimated equilibration half-lives of less than 30 min (results not shown). Overall, modeling showed that subcutaneous tissue and peritoneal fluid were kinetically more similar to the central than to the peripheral compartment (Fig. 2).

The individually fitted meropenem concentrations matched the observed concentrations well (Fig. 1), and the population fitted meropenem concentrations provided unbiased predictions for the average concentrations at all three sites. The model included a major-diagonal variance-covariance matrix and had adequate predictive performance at all three sites as indicated by the visual predictive checks (results not shown).

The concentrations in subcutaneous tissue varied greatly (112% coefficient of variation [CV]) and were, on average, 27.9% lower than those in plasma (F_{SC} = $AUC_{0-\infty}$ in subcutaneous tissue/$AUC_{0-\infty}$ in plasma = 0.721 [$AUC_{0-\infty}$ is the area under the concentration-time curve from 0 h to infinity]). In contrast, concentrations in peritoneal fluid were roughly comparable to those in plasma (F_{PF} = $AUC_{0-\infty}$ in peritoneal fluid/$AUC_{0-\infty}$ in plasma = 0.943), with a moderate between-subject variability of 31.1% CV.

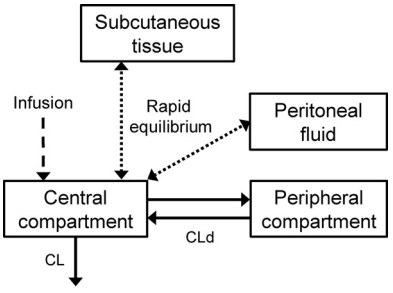

FIG 2 Structure of the final model for meropenem in plasma, subcutaneous tissue, and peritoneal fluid. This model contained a central and a peripheral compartment, as well as compartments for subcutaneous tissue and peritoneal fluid. The latter two compartments were in rapid equilibrium with the meropenem concentrations in the central compartment. CLd, distribution clearance.

A 15-min infusion of 1 g meropenem every 8 h was predicted to achieve greater than 90% probabilities of target attainment up to a MIC of 2 mg/liter in plasma and peritoneal fluid and 0.5 mg/liter in subcutaneous tissue for the 40% $fT_{>MIC}$ target (Fig. 3). As expected, these PK/PD breakpoints were lower (0.25 mg/liter for plasma and peritoneal fluid and 0.125 mg/liter for subcutaneous tissue) when the 75% $fT_{>MIC}$ target was used. For continuous infusion of 3 g/day, these breakpoints were 2 mg/liter for plasma and peritoneal fluid and 0.5 mg/liter for subcutaneous tissue for the 40% and 75% $fT_{>MIC}$ targets. The breakpoints for the 3-h infusion given every 8 h were similar to those for the continuous infusion.

DISCUSSION

The present study is the first to determine meropenem concentrations in the interstitial space fluid of subcutaneous tissue and the peritoneal fluid of obese patients via microdialysis. These sites are highly relevant for infections in these patients. The results of the present study showed that the population PK in plasma was predictable when PK parameters were scaled by fat-free mass (FFM) (Table 2). Contrary to total body weight (WT), FFM accounts for the considerably altered body composition in morbidly obese patients compared to that of nonobese patients (15). As the present study lacked a control group of nonobese patients or of healthy volunteers and had a small sample size, we could not reliably identify whether scaling by FFM or WT was superior.

Our population mean volume of distribution at steady state (27.6 liters) scaled by FFM fell well within the range of estimates from other studies that typically reported 23 to 34 liters in nonobese patients (24–28). This suggested that scaling the volume of distribution by FFM was reasonable. When we used a standard WT of 70 kg for scaling, the volume of distribution at steady state had a relatively small estimate of 16.5 liters. Total meropenem clearance in nonobese patients with normal renal function and in healthy volunteers has been reported to typically fall within 13.5 to 16.1 liters/h (24–27, 29, 30). Our population mean clearance of 18.7 liters/h was slightly outside this range (Table 2). Allometric scaling of clearance by WT resulted in a population mean of 12.7 liters/h for a person with 70 kg WT in our study. Given the substantially altered body composition of morbidly obese patients compared to that of nonobese patients, an allometric body size

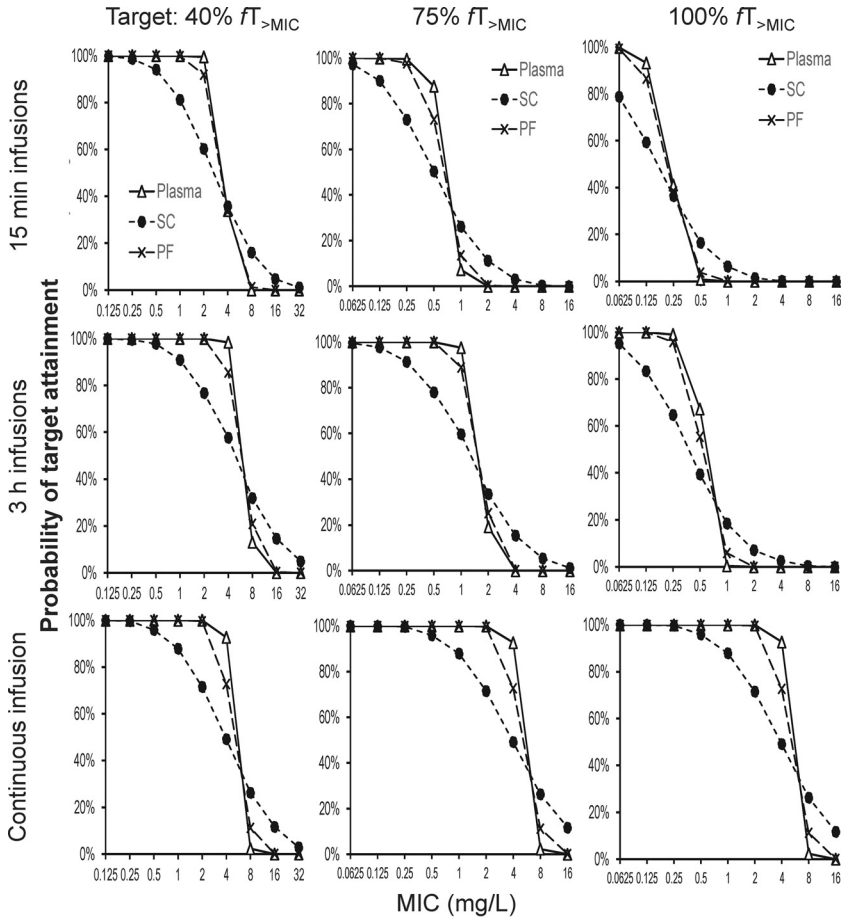

FIG 3 Probabilities of target attainment for 1 g meropenem dosed as a 15-min or 3-h infusion every 8 h or as a continuous infusion with a 1-g loading dose. The PK/PD targets of 40%, 75%, and 100% $fT_{>MIC}$ were assessed for the concentrations in plasma, subcutaneous tissue (SC), and peritoneal fluid (PF).

model based on FFM seemed a plausible approach to predict the PK of meropenem in morbidly obese patients (15). For the 1.8-fold range of FFM and WT between our largest and smallest patient (Table 1), an allometric compared to a linear body size model differs by approximately 15% in the typical clearance and typical terminal half-life over the range of body sizes encountered. Therefore, the difference that justified the choice of an allometric over a linear body size model for our patients was relatively small.

A small number of studies have assessed the PK of meropenem in obese patients (4–8) and modeled the PK data by individual fitting of each profile, but these studies did not utilize population PK modeling. In a therapeutic drug monitoring study (4) with sparse sampling (median of 1 sample per patient), the volumes of distribution were 40.0 liters in obese and 27.9 liters in nonobese patients, and clearance values were 6.06 liters/h in obese and 4.62 liters/h in nonobese patients. These PK parameter estimates were not scaled by body size and were determined in critically ill patients with a wide range of creatinine clearance values (mean, 65 ml/min, and range, 8 to 271 ml/min). Cheatham et al. (8) reported a volume of distribution at steady state of 37.4 ± 14.7 liters and a total clearance of 10.2 ± 5.0 liters/h in nine morbidly obese patients with normal creatinine clearance (107 ± 44 ml/min). Their patients were, on average, 15 years older (55.4 ± 10.1 years) than those in our study (Table 1). A higher volume of distribution of 48.0 ± 25.1 liters and a higher total clearance of 18.0 ± 9.0 liters/h has been reported for noncritically ill obese patients with a creatinine clearance of 107 (range, 6.0 to 389) ml/min and body weight of 103 (81 to 153) kg (5). Overall, after accounting for body size and renal function, our PK parameter estimates (Table 2) in morbidly obese patients were in agreement with the reported range of PK parameter estimates for meropenem in obese patients.

The present study is the first report on the penetration of meropenem in subcutaneous tissue and peritoneal fluid of morbidly obese patients. The penetration of meropenem into subcutaneous tissue varied greatly (112% CV for F_{SC}) (Table 2), and the meropenem AUC in subcutaneous tissue was, on average, 0.721 times the plasma AUC. This population mean estimate was in excellent agreement with the estimates for penetration into subcutaneous tissue calculated via noncompartmental analysis in previous studies (26, 31). However, the between-subject variability for F_{SC} was considerably larger for morbidly obese patients than for the other patients. The penetration of meropenem into peritoneal fluid was rapid, the exposures were roughly comparable to those in plasma, and the between-patient variability of F_{PF} was relatively small (Table 2). The estimated extent of penetration into peritoneal fluid (F_{PF}) in our study was in good agreement with previously reported estimates that ranged from 0.74 to 1.0 (32, 33).

We found that the concentrations in subcutaneous tissue and

peritoneal fluid largely paralleled those in plasma. Population modeling showed a rapid equilibration between these peripheral sites and plasma (Fig. 2; Table 2). Previous studies on the penetration of meropenem into subcutaneous tissue and peritoneal fluid showed rapid equilibration after the end of the infusion (31, 33). Our sampling times ensured that we could adequately characterize the terminal phase and, therefore, the $fT_{>MIC}$.

A limitation of our study is the small sample size of five morbidly obese patients. While it has been shown that this sample size can lead to biased (i.e., too small) estimates for between-patient variability, even five patients yielded unbiased (±1%) and reasonably precise (15.9% coefficient of variation) estimates for clearance (34) and, therefore, for the area under the plasma concentration-time curve. We obtained similar results for the bias and precision of simulated $fT>MIC$ for β-lactams in an exhaustive simulation study (35). While the patients in our study were a typical patient group in our hospital, this small sample size may not cover the full spectrum of morbidly obese patients, which presents a limitation of our study. Additionally, a potential limitation of this study is the application of PK/PD target values that were derived from murine and human plasma concentrations (10), since PK/PD targets for the unbound concentrations in subcutaneous tissue and peritoneal fluid are not available. Despite the limitations associated with the small sample size and the uncertainty associated with the precise PK/PD target values for tissue, our study provides valuable data to guide dosing of meropenem in morbidly obese patients given the lack of population PK data in this patient group.

Our study provides additional information since only two previous studies, with 9 and 10 patients, have assessed the PK of meropenem in morbidly obese patients (7, 8). While our estimated random BSV after accounting for FFM was relatively small (Table 2), the Monte Carlo simulations were performed with a coefficient of variation of 27.4% for FFM (as observed in our patients). This yielded considerable between-patient variability in clearance and volume of distribution for the Monte Carlo simulations.

As expected, the predicted PK/PD breakpoints were comparable for plasma and peritoneal fluid (Fig. 3) and, due to the large variability in F_{SC}, the breakpoints were approximately 4-fold lower for subcutaneous tissue. Importantly, the PK/PD targets for infections in subcutaneous tissue and peritoneal fluid remain to be determined. Therefore, our probabilities of target attainment for subcutaneous tissue and peritoneal fluid should be interpreted conservatively.

In summary, this study presents the first population PK analysis of meropenem in morbidly obese patients. When clearance and volume of distribution were scaled allometrically by FFM, the PK of meropenem was predictable in morbidly obese patients. The penetration of meropenem into subcutaneous tissue and peritoneal fluid was rapid. The concentrations in peritoneal fluid were roughly comparable to those in plasma. However, the subcutaneous tissue concentrations varied greatly and were, on average, 27.9% lower than those in plasma. While this may lead to lower PK/PD breakpoints in subcutaneous tissue than in plasma, further studies are warranted to determine the PK/PD targets at those peripheral sites and to show the clinical benefit of prolonged or continuous versus short-term infusions for intra-abdominal infections and infections of subcutaneous tissue.

ACKNOWLEDGMENTS

J.B.B. is the recipient of a Career Development Fellowship from the Australian National Health and Medical Research Council (NHMRC) (fellowship no. 1084163).

All authors declare no conflict of interest.

REFERENCES

1. **Boucher HW, Talbot GH, Bradley JS, Edwards JE, Gilbert D, Rice LB, Scheld M, Spellberg B, Bartlett J.** 2009. Bad bugs, no drugs: no ESKAPE! An update from the Infectious Diseases Society of America. Clin Infect Dis **48:**1–12. http://dx.doi.org/10.1086/595011.
2. **Infectious Diseases Society of America, Spellberg B, Blaser M, Guidos RJ, Boucher HW, Bradley JS, Eisenstein BI, Gerding D, Lynfield R, Reller LB, Rex J, Schwartz D, Septimus E, Tenover FC, Gilbert DN.** 2011. Combating antimicrobial resistance: policy recommendations to save lives. Clin Infect Dis **52**(Suppl 5)**:**S397–S428. http://dx.doi.org/10.1093/cid/cir153.
3. **Walker B, Barrett S, Polasky S, Galaz V, Folke C, Engstrom G, Ackerman F, Arrow K, Carpenter S, Chopra K, Daily G, Ehrlich P, Hughes T, Kautsky N, Levin S, Maler KG, Shogren J, Vincent J, Xepapadeas T, de Zeeuw A.** 2009. Environment. Looming global-scale failures and missing institutions. Science **325:**1345–1346. http://dx.doi.org/10.1126/science.1175325.
4. **Hites M, Taccone FS, Wolff F, Cotton F, Beumier M, De Backer D, Roisin S, Lorent S, Surin R, Seyler L, Vincent JL, Jacobs F.** 2013. Case-control study of drug monitoring of β-lactams in obese critically ill patients. Antimicrob Agents Chemother **57:**708–715. http://dx.doi.org/10.1128/AAC.01083-12.
5. **Hites M, Taccone FS, Wolff F, Maillart E, Beumier M, Surin R, Cotton F, Jacobs F.** 2014. Broad-spectrum beta-lactams in obese noncritically ill patients. Nutr Diabetes **4:**e119. http://dx.doi.org/10.1038/nutd.2014.15.
6. **Janson B, Thursky K.** 2012. Dosing of antibiotics in obesity. Curr Opin Infect Dis **25:**634–649. http://dx.doi.org/10.1097/QCO.0b013e328359a4c1.
7. **Kays MB, Fleming MR, Cheatham SC, Chung EK, Juenke JM.** 2014. Comparative pharmacokinetics and pharmacodynamics of doripenem and meropenem in obese patients. Ann Pharmacother **48:**178–186. http://dx.doi.org/10.1177/1060028013512474.
8. **Cheatham SC, Fleming MR, Healy DP, Chung EK, Shea KM, Humphrey ML, Kays MB.** 2014. Steady-state pharmacokinetics and pharmacodynamics of meropenem in morbidly obese patients hospitalized in an intensive care unit. J Clin Pharmacol **54:**324–330. http://dx.doi.org/10.1002/jcph.196.
9. **Craig WA.** 1998. Pharmacokinetic/pharmacodynamic parameters: rationale for antibacterial dosing of mice and men. Clin Infect Dis **26:**1–12. http://dx.doi.org/10.1086/516284.
10. **Ambrose PG, Bhavnani SM, Rubino CM, Louie A, Gumbo T, Forrest A, Drusano GL.** 2007. Pharmacokinetics-pharmacodynamics of antimicrobial therapy: it's not just for mice anymore. Clin Infect Dis **44:**79–86. http://dx.doi.org/10.1086/510079.
11. **Stahle L, Arner P, Ungerstedt U.** 1991. Drug distribution studies with microdialysis. III. Extracellular concentration of caffeine in adipose tissue in man. Life Sci **49:**1853–1858.
12. **Koal T, Deters M, Resch K, Kaever V.** 2006. Quantification of the carbapenem antibiotic ertapenem in human plasma by a validated liquid chromatography-mass spectrometry method. Clin Chim Acta **364:**239–245. http://dx.doi.org/10.1016/j.cccn.2005.07.004.
13. **Landersdorfer CB, Kinzig M, Hennig FF, Bulitta JB, Holzgrabe U, Drusano GL, Sorgel F, Gusinde J.** 2009. Penetration of moxifloxacin into bone evaluated by Monte Carlo simulation. Antimicrob Agents Chemother **53:**2074–2081. http://dx.doi.org/10.1128/AAC.01056-08.
14. **Landersdorfer CB, Kinzig M, Bulitta JB, Hennig FF, Holzgrabe U, Sorgel F, Gusinde J.** 2009. Bone penetration of amoxicillin and clavulanic acid evaluated by population pharmacokinetics and Monte Carlo simulation. Antimicrob Agents Chemother **53:**2569–2578. http://dx.doi.org/10.1128/AAC.01119-08.
15. **Janmahasatian S, Duffull SB, Ash S, Ward LC, Byrne NM, Green B.** 2005. Quantification of lean bodyweight. Clin Pharmacokinet **44:**1051–1065. http://dx.doi.org/10.2165/00003088-200544100-00004.
16. **Bauer RJ, Guzy S, Ng C.** 2007. A survey of population analysis methods and software for complex pharmacokinetic and pharmacodynamic models with examples. AAPS J **9:**E60–E83. http://dx.doi.org/10.1208/aapsj0901007.

17. **Bulitta JB, Bingolbali A, Shin BS, Landersdorfer CB.** 2011. Development of a new pre- and post-processing tool (SADAPT-TRAN) for nonlinear mixed-effects modeling in S-ADAPT. AAPS J **13:**201–211. http://dx.doi.org/10.1208/s12248-011-9257-x.
18. **Bulitta JB, Landersdorfer CB.** 2011. Performance and robustness of the Monte Carlo importance sampling algorithm using parallelized S-ADAPT for basic and complex mechanistic models. AAPS J **13:**212–226. http://dx.doi.org/10.1208/s12248-011-9258-9.
19. **Bulitta JB, Duffull SB, Kinzig-Schippers M, Holzgrabe U, Stephan U, Drusano GL, Sorgel F.** 2007. Systematic comparison of the population pharmacokinetics and pharmacodynamics of piperacillin in cystic fibrosis patients and healthy volunteers. Antimicrob Agents Chemother **51:**2497–2507. http://dx.doi.org/10.1128/AAC.01477-06.
20. **Bulitta JB, Okusanya OO, Forrest A, Bhavnani SM, Clark K, Still JG, Fernandes P, Ambrose PG.** 2013. Population pharmacokinetics of fusidic acid: rationale for front-loaded dosing regimens due to autoinhibition of clearance. Antimicrob Agents Chemother **57:**498–507. http://dx.doi.org/10.1128/AAC.01354-12.
21. **Bulitta JB, Zhao P, Arnold RD, Kessler DR, Daifuku R, Pratt J, Luciano G, Hanauske AR, Gelderblom H, Awada A, Jusko WJ.** 2009. Mechanistic population pharmacokinetics of total and unbound paclitaxel for a new nanodroplet formulation versus Taxol in cancer patients. Cancer Chemother Pharmacol **63:**1049–1063. http://dx.doi.org/10.1007/s00280-008-0827-2.
22. **Ariano RE, Nyhlen A, Donnelly JP, Sitar DS, Harding GK, Zelenitsky SA.** 2005. Pharmacokinetics and pharmacodynamics of meropenem in febrile neutropenic patients with bacteremia. Ann Pharmacother **39:**32–38.
23. **Li C, Du X, Kuti JL, Nicolau DP.** 2007. Clinical pharmacodynamics of meropenem in patients with lower respiratory tract infections. Antimicrob Agents Chemother **51:**1725–1730. http://dx.doi.org/10.1128/AAC.00294-06.
24. **Lodise TP, Nau R, Kinzig M, Drusano GL, Jones RN, Sorgel F.** 2007. Pharmacodynamics of ceftazidime and meropenem in cerebrospinal fluid: results of population pharmacokinetic modelling and Monte Carlo simulation. J Antimicrob Chemother **60:**1038–1044. http://dx.doi.org/10.1093/jac/dkm325.
25. **Doh K, Woo H, Hur J, Yim H, Kim J, Chae H, Han S, Yim DS.** 2010. Population pharmacokinetics of meropenem in burn patients. J Antimicrob Chemother **65:**2428–2435. http://dx.doi.org/10.1093/jac/dkq317.
26. **Roberts JA, Kirkpatrick CM, Roberts MS, Robertson TA, Dalley AJ, Lipman J.** 2009. Meropenem dosing in critically ill patients with sepsis and without renal dysfunction: intermittent bolus versus continuous administration? Monte Carlo dosing simulations and subcutaneous tissue distribution. J Antimicrob Chemother **64:**142–150. http://dx.doi.org/10.1093/jac/dkp139.
27. **Li C, Kuti JL, Nightingale CH, Nicolau DP.** 2006. Population pharmacokinetic analysis and dosing regimen optimization of meropenem in adult patients. J Clin Pharmacol **46:**1171–1178. http://dx.doi.org/10.1177/0091270006291035.
28. **Muro T, Sasaki T, Hosaka N, Umeda Y, Takemoto S, Yamamoto H, Kamimura H, Higuchi S, Karube Y.** 2011. Population pharmacokinetic analysis of meropenem in Japanese adult patients. J Clin Pharm Ther **36:**230–236. http://dx.doi.org/10.1111/j.1365-2710.2010.01171.x.
29. **Lodise TP, Sorgel F, Melnick D, Mason B, Kinzig M, Drusano GL.** 2011. Penetration of meropenem into epithelial lining fluid of patients with ventilator-associated pneumonia. Antimicrob Agents Chemother **55:**1606–1610. http://dx.doi.org/10.1128/AAC.01330-10.
30. **Krueger WA, Bulitta J, Kinzig-Schippers M, Landersdorfer C, Holzgrabe U, Naber KG, Drusano GL, Sorgel F.** 2005. Evaluation by Monte Carlo simulation of the pharmacokinetics of two doses of meropenem administered intermittently or as a continuous infusion in healthy volunteers. Antimicrob Agents Chemother **49:**1881–1889. http://dx.doi.org/10.1128/AAC.49.5.1881-1889.2005.
31. **Varghese JM, Jarrett P, Wallis SC, Boots RJ, Kirkpatrick CM, Lipman J, Roberts JA.** 2015. Are interstitial fluid concentrations of meropenem equivalent to plasma concentrations in critically ill patients receiving continuous renal replacement therapy? J Antimicrob Chemother **70:**528–533. http://dx.doi.org/10.1093/jac/dku413.
32. **Ikawa K, Morikawa N, Ikeda K, Ohge H, Sueda T.** 2008. Development of breakpoints of carbapenems for intraabdominal infections based on pharmacokinetics and pharmacodynamics in peritoneal fluid. J Infect Chemother **14:**330–332. http://dx.doi.org/10.1007/s10156-008-0624-1.
33. **Karjagin J, Lefeuvre S, Oselin K, Kipper K, Marchand S, Tikkerberi A, Starkopf J, Couet W, Sawchuk RJ.** 2008. Pharmacokinetics of meropenem determined by microdialysis in the peritoneal fluid of patients with severe peritonitis associated with septic shock. Clin Pharmacol Ther **83:**452–459. http://dx.doi.org/10.1038/sj.clpt.6100312.
34. **Tam VH, Kabbara S, Yeh RF, Leary RH.** 2006. Impact of sample size on the performance of multiple-model pharmacokinetic simulations. Antimicrob Agents Chemother **50:**3950–3952. http://dx.doi.org/10.1128/AAC.00337-06.
35. **Bulitta JB, Lodise TP, Drusano GL, Kinzig-Schippers M, Holzgrabe U, Sörgel F.** 2006. Bias and uncertainty of Monte Carlo simulations with beta-lactams, abstr 969. Abstr 24th Ann Meet Popul Approach Group Eur (PAGE). http://www.page-meeting.org/default.asp?abstr=969.